A Zonal RANS/LES Method for the Flow Around an Airfoil at High Angle of Attack

K.J. Geurts, M. Meinke, and W. Schröder

Abstract. The objective of the current study is the application of a zonal RANS/LES approach to predict the flow field around a HGR-01 airfoil at high angle of attack. In this case a laminar separation bubble with subsequent transition to turbulence and a small trailing edge separation occur. This approach uses an LES zone at the leading edge to capture the laminar separation bubble and a second LES zone at the trailing edge, enclosing the trailing edge recirculation region. The flow in the rest of the computation domain is simulated with a RANS method. Results are presented for a full LES in comparison to experimental data. Good agreement is obtained for the pressure distribution and the location and size of the laminar separation region. First results for the zonal methods show a smooth transition between the RANS and the LES zones and comparable pressure distributions.

1 Introduction

The numerical analysis of flow fields in industrial applications is nowadays mainly based on solutions of the Reynolds-averaged Navier-Stokes equations (RANS). When unsteady flow phenomena like, e.g. local flow separation come into play, turbulence models used to close the RANS equations are often not the appropriate choice to describe complex flow fields. Large Eddy Simulations (LES) are more suitable to accurately predict these phenomena, but they are often too expensive for general industrial applications. Therefore, a zonal RANS-LES method has been developed in which only those flow regions are resolved with LES where the RANS model typically fails to predict the flow field accurately. In this study, which is part of the ComFliTe research project coordinated by DLR Braunschweig, the zonal method is applied to the prediction of the unsteady flow behavior of the HGR-01

K.J. Geurts · M. Meinke · W. Schröder
Institute of Aerodynamics, RWTH Aachen University, Wüllnerstr. 5a,
52062 Aachen, Germany
e-mail: k.geurts@aia.rwth-aachen.de

A. Dillmann et al. (Eds.): *New Results in Numer. & Exp. Fluid Mech.*, NNFM 121, pp. 465–472.
DOI: 10.1007/978-3-642-35680-3_55

research airfoil close to stall, where a laminar separation bubble (LSB) at the leading edge and turbulent trailing edge separation occur [10]. The goal of this study is to validate and check the applicability of the fully coupled zonal RANS/LES method for the determination of airfoil characteristics at high angles of attack, when first separated flow regions occur.

2 Numerical Simulation Methods

2.1 Large-Eddy Simulation

The Navier-Stokes equations for three-dimensional compressible flows are solved by a block-structured finite-volume flow solver. A modified AUSM method is used for the Euler terms which are discretized to second-order accuracy by an upwind-biased approximation. For the non-Euler terms a centered approximation of second-order accuracy is used. The temporal integration is done by a second-order accurate explicit 5-stage Runge-Kutta method, the coefficients of which are optimized for maximum stability. For a detailed description of the flow solver the reader is referred to Meinke *et al.* [6] and the references therein. The sub-grid scale modeling for the large-eddy simulations is based on an implicit method, i.e., the MILES (monotone integrated LES).

2.2 Zonal RANS/LES Computation

A detailed overview of the different zonal RANS/LES methods was given by Fröhlich *et al.* [3]. In the scope of the ComFliTe research project, a zonal method is applied in which segregated solvers are used in the RANS and LES zones. An uncoupled version of such a zonal RANS/LES method was already successfully applied to determine the flow field for a high-lift wing-flap airfoil configuration [11]. The zonal method applied for the HGR-01 airfoil at high angle of attack is based on two LES regions embedded in a large RANS domain. The two LES regions are used to resolve the flow at the leading and trailing edge region where flow separation occurs, while the RANS zone is used for the attached flow regions. The flow variables are transferred between the two methods. The schematics of the overlapping zones is shown in Figure 1.

In the overlapping region, where the flow is directed from a RANS to LES zone, synthetic eddies are introduced to accelerate the generation of coherent turbulent structures using the method of Jarrin *et al.* [4]. Furthermore, control planes are used to to drive the solution towards the correct turbulence level in the LES domain according to Spille and Kaltenbach [8]. When going from the LES domain to the RANS domain, the eddy viscosity ν_t is reconstructed from time and spatial averaging of the LES data. More details of the coupling method are given in the following two sections.

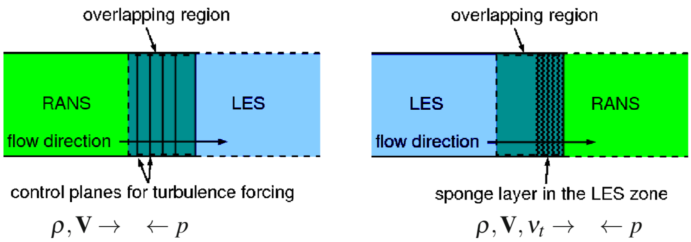

Fig. 1 Schematic overview of the overlapping regions between the RANS and LES regions. Here ρ denotes the density, $\mathbf{V}$ the velocity vector, p the pressure and ν_t the turbulent eddy viscosity, respectively.

2.2.1 Transition from RANS to LES

At the LES inlet synthetic turbulence is specified to provide a reasonable estimate of the fluctuating turbulent velocity field. The method of Jarrin *et al.* [4] is based on considering turbulence as a superposition of coherent structures. These structures are generated in the LES inlet plane and are defined by a shape function which describes the spatial and temporal characteristics of the turbulent structure.

The required turbulent length and time scales are determined by the Reynolds shear stress component $\langle u'v' \rangle$ which is reconstructed by using the turbulent viscosity ν_t provided by the corresponding RANS solution. The turbulent time scale can be written as $t{=}k/\varepsilon$ and the turbulent length scale as $L{=}t\ V_b$ where $V_b{=}\sqrt{k}$ and k and ε represent the turbulent kinetic energy and turbulent dissipation, respectively. By applying the experimental correlation of Bradshaw *et al.* [1], the turbulent kinetic energy is related to the Reynolds shear stress $\langle u'v' \rangle$ and furthermore is the turbulent viscosity ν_t readily available from the RANS solution. In this study, the Spalart-Allmaras turbulence model [7] was used for the RANS domain.

The synthetic turbulent method, described above, provides a reasonable first estimate of the fluctuating turbulent velocity field. Downstream of the inlet boundary, however, the relevant turbulent scales may vanish due to the fact that the fluctuations are not a solution of the Navier-Stokes equations. Therefore, control planes are used in which a volumetric forcing term is introduced into the Navier-Stokes equations to regulate the turbulent production in the shear stress budget [8]. As discussed in the work of Zhang *et al.* [11], local flow events such as bursts and sweeps are enhanced or damped by the local forcing thus contributing to the Reynolds shear stress $\langle u'v' \rangle$ to attain a target Reynolds shear stress at the control plane which is provided by the RANS solution.

2.2.2 Transition from LES to RANS

Following the work of König *et al.* [5], the eddy viscosity is determined by the ratio of the turbulent kinetic energy k, over the turbulent frequency ω. The quantity ω is approximated by a generalized form of Bradshaw's hypothesis [1] using the norm of the mean strain tensor. It is obvious that this method just needs the normal components of the Reynolds stress tensor to compute the turbulent kinetic energy k. The computation of the turbulent frequency ω requires only the derivatives of mean velocities and not of their fluctuations. A detailed discussion of the method is given in König *et al.* [5]. Furthermore, time averaged values for the velocity and density are transmitted to the inflow boundary of the RANS domain.

3 Flow and Computation Parameters

The airfoil profile in this study is the research airfoil known as HGR-01. This airfoil is designed to have a mixed stall behavior of leading edge and trailing edge stall [10]. Specific to this airfoil is that the trailing edge separation is moving upstream from the trailing edge before full stall occurs.

An extensive database of experimental results is available and the chosen test configuration for this study has a Reynolds number of $0.6565 \cdot 10^6$ and an angle of attack of 12^o at the low speed Mach number of 0.15.

The full LES computation that will serve as a reference for the further zonal computations uses a C-type grid consisting of 32 structured blocks. Cell sizes were chosen to resolve the near wall region with maximal values of $\Delta x^+ \approx 30$, $\Delta y^+ \approx 1$ and $\Delta z^+ \approx 20$ where x, y, z are the streamwise, wall normal and spanwise direction respectively. This results in a total number of grid points of of $51 \cdot 10^6$ where 100 points are spread over the 2 % chord length extension in spanwise direction. Figure 2 shows a plane normal to the spanwise direction of the LES grid. From the mesh for the full LES two separate LES zones are cut out around the leading and trailing edge area for the zonal RANS/LES solution, where flow separation occurs. In Figure 3 these LES zones are shown in red color. Around the LES zones a RANS domain is defined which is shown in black in the same Figure and overlaps as required with the LES domain. In this overlap the flow variables of the different turbulence model regions are transferred as described in section 2.2. Cell sizes for the RANS domain result in maximal values of $\Delta x^+ \approx 500$, $\Delta y^+ \approx 1$ and $\Delta z^+ \approx 200$. Using the zonal method for the HGR-01 profile, a factor 4 in grid points is saved, resulting in a corresponding reduction of computation time.

4 Results

4.1 Full Large Eddy Simulation

The purpose of the full LES computation is to obtain a reference solution for the zonal method. Using available experimental results, the ability of the LES computation to capture the relevant unsteady flow phenomena is investigated.

The results shown in Figure 6 for the pressure coefficient show that both goals are reached. As can be seen by the comparison of the pressure coefficient with the experimental data, the LES computation delivers an accurate result with respect to the position and size of the LSB. The turbulent kinetic energy at the leading edge, together with the dividing streamline is presented in Figure 5, to show the transition

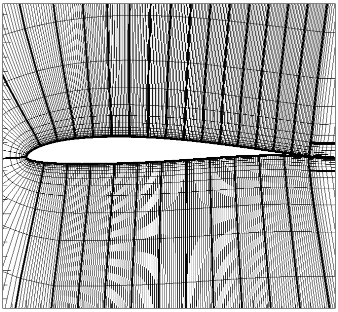

Fig. 2 Structured C-grid (32-blocks) for the full LES. The total number of points is $51 \cdot 10^6$.

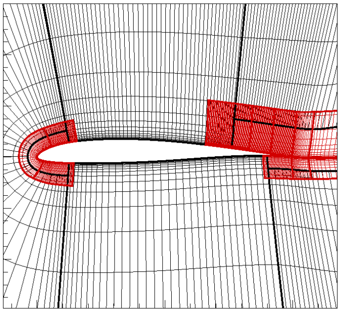

Fig. 3 Grid used for the zonal RANS/LES solution. The mesh is composed of 16-blocks and the total number of points is $13 \cdot 10^6$. The LES zones are plotted in red.

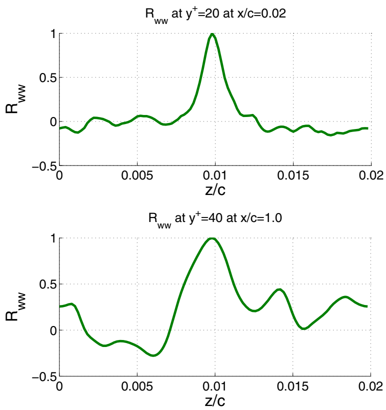

Fig. 4 Two-point correlation of the spanwise velocity fluctuations R_{ww} in spanwise direction z/c near reattachment of the laminar separation bubble and in the recirculation region at the trailing edge

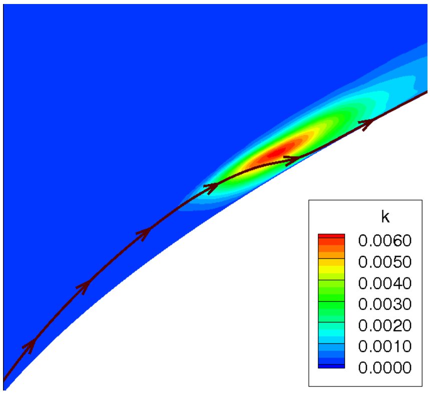

Fig. 5 Distribution of the turbulent kinetic energy k around the leading edge of the airfoil indicating the transition to turbulence in the LSB

from the laminar to a turbulent boundary layer state. The streamline curvature near the reattachment point is causing a peak in turbulence production and the turbulent kinetic energy [2]. While the lift coefficient (1.366) compares well with the experimental data (1.370), the drag is overpredicted. The experiments result in a drag coefficient of 0.032, whereas the full LES computation delivers the value 0.0403. A possible explanation for that is the size of the trailing edge separation. As Touber and Sandham [9] explain, a domain with a two small extent in spanwise direction can lead to non-vanishing correlations in spanwise direction. This effect can lead to a too large separation bubble increasing the pressure drag. To analyze whether the used span of 2 % chord length is sufficient to capture all three-dimensional effects correctly in the present simulation, the two-point correlation of the spanwise velocity fluctuations were computed at different positions over the airfoil chord. From the upper Figure 4, where the two-point correlation in the LSB at $y^+ = 20$ is shown, it can be seen that the correlation from the center line drops to zero within approx. 1% of the chord length. This indicates that the spanwise extent is sufficiently large to accurately describe the turbulent flow in the vicinity of the LSB. The lower Figure 4 shows the two-point correlation at $y^+ = 40$ in the trailing edge recirculation zone. Obviously, the two-point correlation does not fully drop to zero within the domain. This indicates that a larger span might be required to correctly capture the trailing edge separation. A further increase of the domain extent leads to huge computational effort. Therefore, investigations will be carried out with the zonal RANS/LES method after its validation.

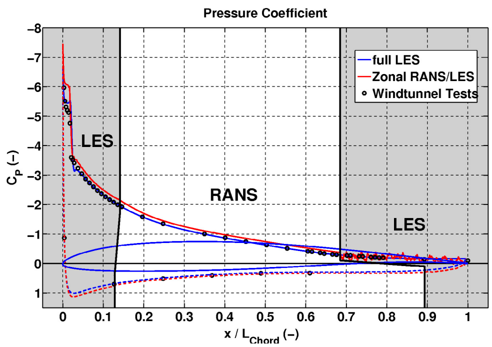

Fig. 6 Comparison of the pressure coefficient c_P for LES and zonal computations and the experimental results [10]

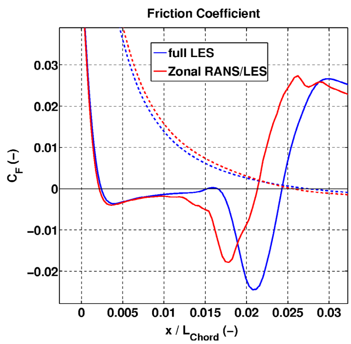

Fig. 7 Close-up of the friction coefficient at the leading edge

4.2 *Zonal RANS/LES*

The purpose of the applied zonal RANS/LES computations is to reduce calculation time and cost, but to maintain the same accuracy as what is achieved with a full LES. The most important values for airfoils at high angle of attack where recirculation regions come into play are the results for the friction and pressure coefficients. Figure 7 shows a close-up of the friction coefficient at the leading edge to visualize the existence and the size of the LSB in both the LES and zonal computations. Figures 8 and 9 show Mach number contour plots for both the LES and zonal RANS/LES computations. The laminar separation bubble is clearly visible in both cases as the blue region on top of the leading edge indicates the recirculating flow. This proofs the ability to capture this phenomenon with the use of the zonal method. Furthermore, a smooth transition from the RANS to the LES domain is visible in

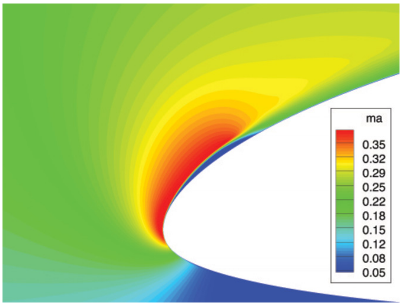

Fig. 8 Mach number contour plot of the leading edge and LSB computed with full LES

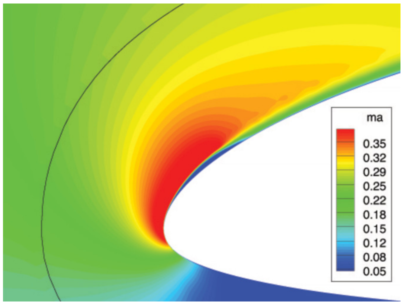

Fig. 9 Mach number contour plot and LSB computed with zonal RANS/LES. The black line indicates the boundary of the LES region.

Figure 9, where the black line indicates the outflow boundary of the RANS domain. Figure 6 presents the pressure distribution of the full LES and experiments, together with the pressure distribution of the zonal RANS/LES solution. It can be seen that the curve has a smooth and continuous transition between the LES and RANS domains. The interface location between RANS and LES is indicated by short vertical black lines in the pressure distribution. The 5 drop in pressure coefficient at about 3% chord length indicates the reattachment point and shows that the size of the LSB is accurately reproduced also by the zonal solution. However, the pressure value in the laminar separation is clearly higher than that in the full LES and the experiments. This is due to fact that the zonal solution has not yet reached a fully developed state so that the simulation has to run a longer time before correct time averaged results and turbulence statistics can be obtained.

5 Conclusion

This paper presents both results of full LES and zonal RANS/LES in comparison to experimental data for the flow around the HGR-01 profile at high angles of attack. This test case is a challenge especially for the turbulence modeling due to the existence of a laminar separation bubble and a small separated flow region at the trailing edge. It is shown that the full LES computation leads to an accurate prediction of both phenomena, but may require a sufficient extent of the domain in spanwise direction to capture correctly the size of the trailing edge separation.

When it comes to the zonal RANS/LES computation, it is shown that for this test case, the boundary conditions and the overlap of the different computational domains result in a smooth and continuous transition of the flow variables. The zonal RANS/LES approach is able to capture the flow phenomena such as the laminar separation bubble with subsequent transition. The presently available results, however, are not fully converged yet. More samples are still required for obtaining smooth statistical data of the turbulent flow field. With these samples a more detailed validation of the zonal RANS/LES will be carried out.

Acknowledgements. The work and results presented in this paper have been conducted within the ComFliTe project sponsored by BMWi.

References

1. Bradshaw, P., Ferriss, D.H., Atwell, N.P.: Calculation of Boundary Layer Development using the Turbulent Energy Equation. J. Fluid Mech. 23, 31–64 (1967)
2. Burgmann, S.: Investigation of Transitional Separation Bubbles using Three-Dimensional Measurement Techniques, Dissertation RWTH Aachen University (2009)
3. Fröhlich, J., Von Terzi, D.: Hybrid RANS/LES Methods for the Simulation of Turbulent Flows. Progress in Aerospace Sciences 44, 349–377 (2008)
4. Jarrin, N., Benhamadouche, N., Laurence, S., Prosser, D.: A synthetic-eddy-method for generating inflow conditions for large-eddy simulations. Journal of Heat and Fluid Flow 27, 585–593 (2006)
5. König, D., Schröder, W., Meinke, M.: Embedded LES-to-RANS boundary in zonal simulations. Journal of Turbulence 11(7), 1–25 (2010)
6. Meinke, M., Schröder, W., Krause, E., Rister, T.: A Comparison of Second- and Sixth-Order Methods for Large-Eddy Simulations. Computers and Fluids 31, 695–718 (2002)
7. Spalart, P.R., Allmaras, S.R.: A One-Equation Turbulence Model for Arodynamic Flows. AIAA Paper 92-0439 (1992)
8. Spille, A., Kaltenbach, H.-J.: Generation of turbulent inflow data with a prescribed shear-stress profile. In: Third AFSOR Conference on DNS and LES (2001)
9. Touber, E., Sandham, N.D.: Large-eddy simulation of low-frequency unsteadiness in a turbulent shock induced separation bubble. Theor. Comput. Fluid Dyn. 23, 79–107 (2009)
10. Wokoeck, R., Krimmelbein, N., Ortmanns, J., Ciobaca, V., Radespiel, R., Krumbein, A.: RANS Simulation and Experiments on the Stall Behaviour of an Airfoil with Laminar Separation Bubbles. AIAA Paper (2006), AIAA-2006-0244
11. Zhang, Q., Schröder, W., Meinke, M.: A zonal RANS-LES method to determine the flow over a high-lift configuration. Computers and Fluids 39(7), 1241–1253 (2010)